




# Extra-Axial Inflammatory Signal in Parameninges in Migraine with Visual Aura

Nouchine Hadjikhani, MD, PhD , Daniel S. Albrecht, PhD , Caterina Mainero, MD, PhD, Eri Ichijo, MS , Noreen Ward, MS, Cristina Granziera, MD, PhD, Nicole R. Zürcher, PhD, Oluwaseun Akeju, MD, Guillaume Bonnier, PhD, Julie Price, PhD, Jacob M. Hooker, PhD, Vitaly Napadow, PhD, Matthias Nahrendorf, MD, PhD, Marco L. Loggia, PhD,<sup>†</sup> and Michael A. Moskowitz, MD<sup>†</sup>

**Objective:** Cortical spreading depression (CSD) underlies the neurobiology of migraine with aura (MWA). Animal studies reveal networks of microvessels linking brain–meninges–bone marrow. CSD activates the trigemino-vascular system, evoking a meningeal inflammatory response. Accordingly, this study examines the upregulation of an inflammatory marker in extra-axial tissues in migraine with visual aura.

**Methods:** We used simultaneously acquired <sup>11</sup>C-PBR28 positron emission tomography/magnetic resonance imaging data of 18kDa translocator protein (an inflammatory marker) in MWA patients (n = 11) who experienced headaches and visual aura in the preceding month. We measured mean tracer uptake (standardized uptake value ratio [SUVR]) in 4 regions of interest comprising the meninges plus the adjacent overlying skull bone (parameningeal tissues [PMT]). These data were compared to healthy controls and patients with pain (chronic low back pain).

**Results:** MWA had significantly higher mean SUVR in PMT overlying occipital cortex than both other groups, although not in the PMT overlying 3 other cortical areas. A positive correlation was also found between the number of visual auras and tracer uptake in occipital PMT.

**Interpretation:** A strong persistent extra-axial inflammatory signal was found in meninges and calvarial bone overlying the occipital lobe in migraine with visual auras. Our findings are reminiscent of CSD-induced meningeal inflammation and provide the first imaging evidence implicating inflammation in the pathophysiology of migraine meningeal symptoms. We suspect that this inflammatory focus results from a signal that migrates from underlying brain and if so, may implicate newly discovered bridging vessels that crosstalk between brain and skull marrow, a finding of potential relevance to migraine and other neuroinflammatory brain disorders.

ANN NEUROL 2020;87:939–949

## Introduction

According to the World Health Organization, migraine is the 6th most prevalent medical disorder on the planet in terms of global burden of disease.<sup>1</sup> Migraine with aura (MWA) constitutes approximately 25% of cases, and the aura, which most often anticipates the headache, may be visual (>90%), sensory, speech, or motor. Migraine patients also experience symptoms such as photophobia

suggesting the presence of meningeal inflammation or irritation.

Cortical spreading depression (CSD) underlies migraine with visual aura (Hadjikhani et al;<sup>2</sup> for review see Pietrobon and Moskowitz<sup>3</sup>). CSD is a slow (2–5mm/min), self-propagating wave of nearly complete depolarization of neurons and glia that is easily evoked in cortical gray matter.<sup>3</sup> Furthermore, CSD triggers an inflammatory response in

View this article online at [wileyonlinelibrary.com](https://www.wileyonlinelibrary.com). DOI: 10.1002/ana.25731

Received Nov 20, 2019, and in revised form Feb 20, 2020. Accepted for publication Mar 22, 2020.

Address correspondence to Dr Moskowitz, Departments of Neurology and Radiology, 149 13th Street, Charlestown, MA 02129.

E-mail: [moskowitz@helix.mgh.harvard.edu](mailto:moskowitz@helix.mgh.harvard.edu)

<sup>†</sup>M.L.L. and M.A.M. contributed equally.

From the Massachusetts General Hospital, Harvard Medical School, Charlestown, MA, USA

brain and meninges. It sensitizes and activates trigeminal afferents within meninges,<sup>4–6</sup> the only nociceptor-containing tissue within the cranium.

Although suspected, meningeal inflammation has never been documented in a population of migraineurs. Most clinical studies in migraineurs measure blood flow, vessel caliber, or blood oxygen level dependent responses within brain, and rarely within meninges, hence the importance and novelty of this study using a 2nd generation positron emission tomography (PET) ligand,<sup>11</sup>C-PBR28, that detects activated inflammatory cells (reviewed in Albrecht et al,<sup>7</sup> Nutma et al<sup>8</sup>). Its binding site, the 18kD translocator protein (TSPO), is located on outer mitochondrial membranes. Previously known as the peripheral benzodiazepine receptor, TSPO, expressed at low levels in healthy central nervous system (CNS) tissue, is often used as a marker of glial activation within brain parenchyma,<sup>9,10</sup> reflecting activated microglia and/or astrocytes in multiple animal models of disease as well as humans.<sup>8,11,12</sup>

In addition, TSPO is upregulated in activated macrophages and other peripheral immune cells,<sup>13</sup> and therefore can also be used as an imaging marker of peripheral inflammation. Our group recently published a clinical report in MWA showing increased <sup>11</sup>C-PBR28 uptake in pain processing pathways, including the thalamus, the primary and secondary somatosensory and insular cortices, and the spinal trigeminal nucleus, as well as in occipital areas shown to be involved in CSD generation.<sup>14</sup> Notably, in a rat CSD model, elevated TSPO signal was sustained for at least 15 days in ipsilateral hemisphere,<sup>15</sup> not unlike what we recently observed in primary visual cortex in migraineurs.<sup>14</sup>

Here we examined parameningeal tissues (PMT) by simultaneous PET/magnetic resonance imaging (MRI) using <sup>11</sup>C-PBR28 in humans with migraine visual auras. Data from the same pool of participants reported in Albrecht et al<sup>14</sup> were further analyzed here to specifically investigate PMT, including meninges and bone marrow, and their relationship to the underlying brain. We sought to determine whether there was a robust inflammatory signal in PMT overlying occipital lobe as anticipated from numerous preclinical data. We compared results to regions remote from visual cortex and compared results to either chronic pain patients (chronic low back pain [CLBP]) or healthy controls. We also examined whether the elevated uptake in occipital PMT correlated with the number of visual auras and determined the impact of time since last attack on signal intensity.

The data show that parameningeal inflammation overlying visual cortex is a consistent phenotype in migraine with visual aura. This phenotype may explain

the symptoms of meningeal irritation in migraineurs and provide further insights into migraine pathophysiology.

## Subjects and Methods

All participants gave written informed consent, and the protocol was approved by the institutional review board of Partners Healthcare.

### Participants

Among 40 subjects initially responding to a questionnaire, 13 patients were entered into the study (10 females; mean age = 31.15 years, range = 18–65). They all fulfilled the International Headache Society criteria for MWA,<sup>16</sup> suffered from episodic migraine (<15 headache days per month), and kept a diary where they reported (1) days (date) when they were experiencing a migraine (with or without aura), (2) the time when the attack started, (3) the severity of the attack, (4) the presence or not of nausea/vomiting, as well as (5) medications taken. The diary was kept for at least 4 weeks prior to PET/MRI imaging. During enrollment, patients were also interviewed about the quality of their migraine attacks, including whether they usually experienced nausea, phonophobia, and photophobia, and the characteristics of the aura they would typically experience. They were also interviewed about their migraine history (number of years, frequency, length of crises, triggers) and their usual medication. Prior to the scanning session, patients discussed in a second interview the content of their diary including information about the presence/absence of auras. For the present study, we only considered migraineurs who had at least 1 migraine with visual aura during the previous 4 weeks, resulting in the inclusion of 11 of the 13 patients in the final analyses.

During an initial screening visit, a blood sample was obtained to genotype subjects for the Ala147Thr *TSPO* polymorphism, which is known to affect binding affinity for <sup>11</sup>C-PBR28.<sup>17</sup> Low-affinity binders (Thr/Thr) were excluded from participation. Only high-affinity binders (HABs; Ala/Ala) and mixed-affinity binders (MABs; Ala/Thr) were included. Exclusion criteria for migraineurs were contraindications for PET or MRI scanning (eg, pregnancy, claustrophobia, ferromagnetic implants, benzodiazepines). The final group of patients consisted of 11 individuals (1 male; mean age = 29.6 years, range = 18–65). Seven of these 11 participants were HABs, and 4 were MABs.

Every patient experienced at least 1 episode of migraine headache in the previous 4 weeks of observation (median number of attacks = 3, range = 1–11). One patient (#113) experienced a migraine headache with no aura starting during the scanning session but did complete the study. The median number of visual auras experienced was 3 per patient (range = 1–6), and aura symptoms were either purely visual or a combination of visual, sensory, language, and cognitive. Auras lasted for <1 hour. Descriptions of the visual auras included spots, glitters, blurred vision, scotoma, partial field cut, and classical visual aura.<sup>18</sup> During attacks, 11 patients experienced photophobia, 10 noted phonophobia, and about one-half reported feeling nauseated. Except for Patient #113 (as noted above), migraine subjects were

pain-free during the imaging study. For our patient population, the median number of days between the last attack and the scanning session was 8 days, and the longest interval between an attack and the scanning session was 18 days (Patient #112).

None of the migraineurs was taking preventive medication, and they refrained from taking nonsteroidal anti-inflammatory drugs (NSAIDs) in the 2 weeks preceding the scanning session. Clinical details of individual migraineurs can be found in the Table and in Albrecht et al.<sup>14</sup>

**Protocol**

The timing of the protocol was chosen based on a report in rodents, where a published study found higher TSPO uptake at 15 days after CSD than at earlier time points (later points were not examined).<sup>15</sup> We instructed patients to keep a diary for 2 weeks, and to call us when they had a migraine attack. Based on this call, we could schedule an imaging session approximately 2 weeks later. Some did not have any more episodes after calling us (e.g., patients #109, #112,

and #123), whereas others had several more attacks. Our primary aim was to determine whether there was a robust PET signal enhancement in this population with multiple auras.

We compared data from 11 migraineurs with aura to data from 2 other groups with similar age range and matched for binding affinity: 11 healthy controls (CON; 7 HABs; 6 males; mean age = 34.9 years, range = 22–52) and 11 patients suffering from CLBP (7 HABs; 3 males; mean age = 45.9 years, range = 27–63). All CLBP patients had a diagnosis of back pain (either with or without radicular pain complaints) dating at least 2 years prior to enrollment and no history of major medical disorders and were not on benzodiazepines or blood thinners. Opioids were allowed only if at low or moderate doses (<60mg morphine equivalents). Healthy controls had the same inclusion/exclusion criteria as the patients, except that they were required not to have a history of migraine or CLBP.

The CLBP cohort was included to evaluate whether any changes observed in the MWA patients are specific to migraine

**TABLE. Patients' Clinical Characteristics**

| ID  | Binding Affinity | Sex | Age, yr | Aura Type   | Frequency | Total Attacks, n | Headaches without Aura, n | Auras, n | Days before Scan, n |
|-----|------------------|-----|---------|---|-----------|------------------|---------------------------|----------|---------------------|
| 104 | HAB              | F   | 27      | Visual + slurred speech   | 2–6       | 3                | 0                         | 3 (3/0)  | 4                   |
| 105 | HAB              | F   | 22      | Visual + vertigo  | 10–15     | 3                | 0                         | 3 (1/2)  | 4                   |
| 109 | MAB              | F   | 30      | Visual + sensory symptoms + aphasia                             | 2         | 4                | 0                         | 4 (4/0)  | 14                  |
| 112 | HAB              | F   | 35      | Visual + sensory symptoms + slurred speech                      | 1–3       | 3                | 0                         | 3 (3/0)  | 18                  |
| 113 | MAB              | M   | 37      | Visual  | 1–3       | 11               | 8                         | 3 (3/0)  | 0                   |
| 114 | HAB              | F   | 22      | Visual  | 3–4       | 2                | 0                         | 2 (2/0)  | 7                   |
| 116 | MAB              | F   | 23      | Visual + speech disturbances + confusion                        | 2–3       | 5                | 2                         | 3 (0/3)  | 2                   |
| 118 | HAB              | F   | 65      | Visual + confusion, difficulty finding words + sensory symptoms | 8         | 5                | 3                         | 2 (2/0)  | 9                   |
| 123 | HAB              | F   | 23      | Visual + sensory symptoms                                       | 1         | 1                | 0                         | 1 (1/0)  | 14                  |
| 125 | MAB              | F   | 23      | Visual + confusion, anxiety + sensory symptoms                  | 1         | 3                | 0                         | 3 (3/0)  | 9                   |
| 126 | HAB              | F   | 18      | Visual + slurred speech   | 3         | 7                | 1                         | 6 (6/0)  | 8                   |

All 11 patients experienced photophobia; 10 patients had phonophobia (all but Patient #112). Age indicates age at scan. Aura Type refers to type of aura experienced by the patient before a migraine attack, as reported in their migraine history. Frequency indicates reported history of migraine frequency per month. Total Attacks indicate total number of migraine attacks in the 4 weeks preceding the scan. Headaches without Aura is the number of headaches during the 4 weeks preceding the scan that were not accompanied by a visual aura. Auras refer to the number of auras (with/without headache, in parentheses) during the 4 weeks preceding the scan. Days before Scan are the number of days between the last migraine attack and the scan.

F = female; HAB= high-affinity binder; M = male; MAB = mixed-affinity binder.

or represent a more general feature common to disorders accompanied by pain, regardless of etiology. There were more females in the migraine cohort, reflecting the higher female prevalence of migraine and the availability of qualified subjects. There were no significant differences in demographics between CLBP and CON, or between CON and MWA, although a 1-way analysis of variance (ANOVA) showed a significant difference in age between the 3 groups ( $F = 4.6$ ,  $p = 0.02$ ), and post hoc Tukey multiple comparison showed that the CLBP subjects were older than migraineurs. CLBP subjects had back pain with or without a radicular component and reported on average pain during the scan of  $31.5 \pm 24.6$  (standard deviation) on a 0 to 100 numerical rating scale. Neither CLBP patients nor CON reported a history of migraine during the history and physical examination.

### Image Acquisition

The PET data were acquired on a prototype MRI-compatible brain PET scanner (BrainPET) designed to fit inside the Magnetom Tim Trio 3 T MRI scanner (Siemens Healthcare, Erlangen, Germany). Structural T1 images were acquired prior to radiotracer injection. Dynamic PET acquisition started concurrently with an injected intravenous bolus of  $^{11}\text{C}$ -PBR28, and data were stored in listmode format. T1 images were used for the generation of attenuation correction maps<sup>19</sup> as well as anatomical localization and spatial normalization of the PET data.

### Data Processing and Analysis

Analytic details are described in Albrecht et al,<sup>14</sup> except that here skull/meninges were not masked out (as customary in brain imaging studies), but rather used to create regions of interest (ROIs). Briefly, standardized uptake value (SUV) images (60–90 minutes after  $^{11}\text{C}$ -PBR28 administration) were generated, coregistered to the magnetization-prepared rapid gradient echo, nonlinearly transformed into Montreal Neurological Institute (MNI) space, and smoothed with a 2mm full width half maximum Gaussian kernel, using a combination of FMRIB Software Library (FSL; <https://fsl.fmrib.ox.ac.uk/fsl/fslwiki>), FreeSurfer (<https://surfer.nmr.mgh.harvard.edu/>), and SPM tools (<https://www.fil.ion.ucl.ac.uk/spm/>). Voxelwise SUV ratio (SUVR) images were obtained by dividing SUV images by average SUV from a pseudoreference region, as previously described.<sup>14</sup> Data were first examined in subjects' native space (ie, before transformation into MNI space).

Anatomical ROIs were created manually on the average MNI brain in FSL, in the meninges/skull marrow over the convexity. They were then automatically applied as a mask on the MNI-normalized brain of each individual subject. These ROIs included the skull marrow as well as the inner periosteum of the skull (dura mater). These 2 tissues were not discernible by PET due to low inherent imaging resolution; for this reason, we use the term PMT. The ROIs were drawn to test the hypothesis that an enhanced binding signal would be detected within tissues overlying the brain, especially within bone marrow. The ROI covered the PMT over the visual cortex, the orbitofrontal cortex,

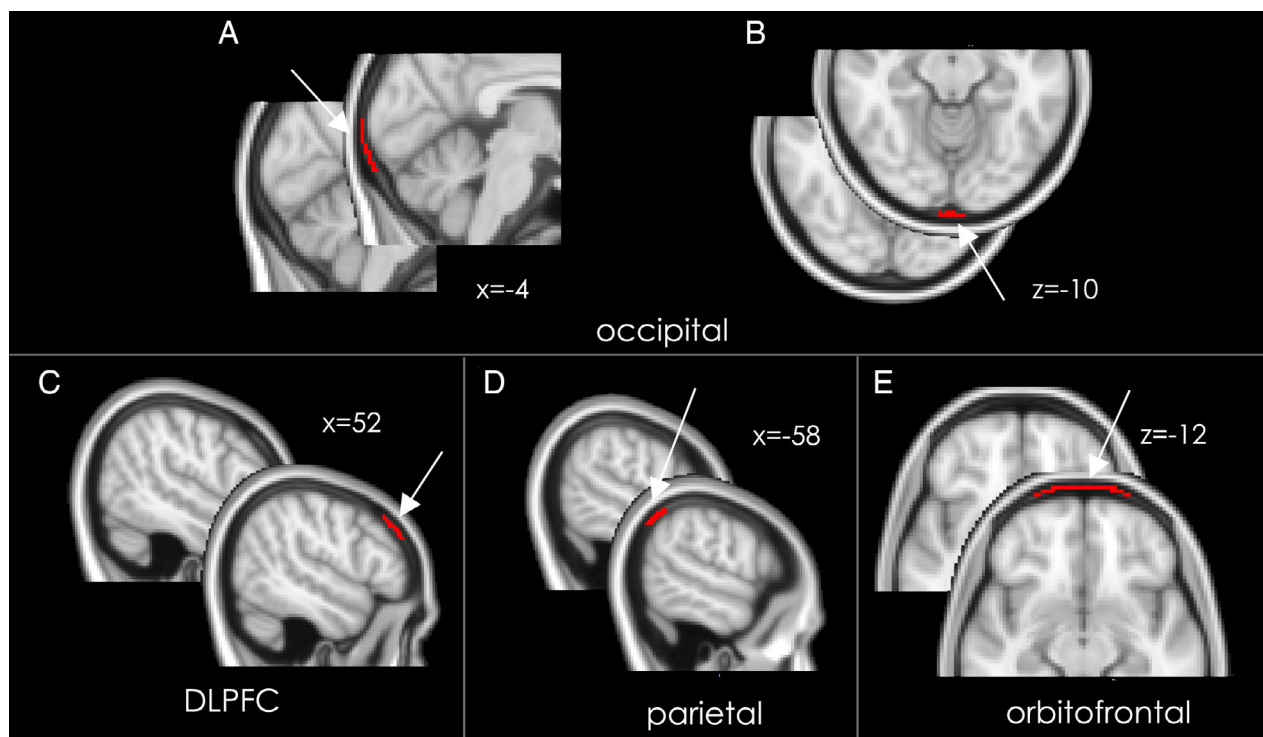


**FIGURE 1:** Meninges/skull bone marrow regions of interest (ROIs). The ROI locations are indicated by arrows and red lines, and the native image is shown next to each ROI to indicate the parameningeal tissue area. A and B show the occipital meninges/skull ROI and C–E the control ROIs, on the Montreal Neurological Institute (MNI) 152 brain template. (C) Dorsolateral prefrontal cortex (DLPFC). (D) Parietal. (E) Orbitofrontal. Each ROI contained 100 voxels; x and z refer to the MNI coordinates of the slices shown in each panel. [Color figure can be viewed at [www.annalsofneurology.org](http://www.annalsofneurology.org)]

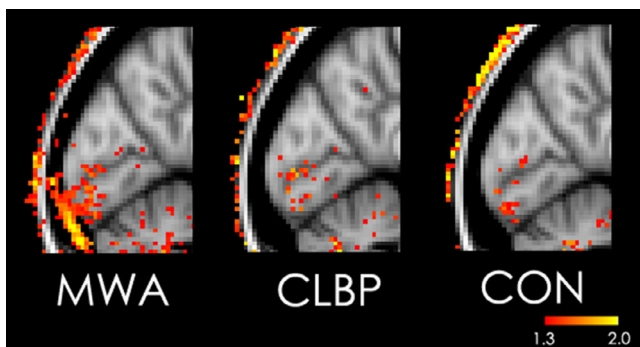


**FIGURE 2:** Standardized uptake value ratio in the occipital cortex and PMT in the average data for each group, on the Montreal Neurological Institute 125 brain template. CLBP = chronic low-back pain patients; CON = healthy controls; MWA = migraineurs with aura. [Color figure can be viewed at [www.annalsofneurology.org](http://www.annalsofneurology.org)]

the dorsolateral prefrontal cortex (DLPFC), and the parietal cortex. All ROIs had the same volume (100 voxels). ROIs were chosen based on their proximity to occipital lobe (parietal lobe), their relation to sensory processing and modulation (DLPFC), or as a negative or neutral reference (orbitofrontal cortex; Fig 1).

Using fslmaths, an FSL tool, SUVRs were automatically extracted from these ROIs in all 3 groups. The FSL tool fslstats was used to calculate the mean SUVR in all the ROIs and to create a histogram showing the distribution of values, with 10 bins from 0.3 to 3.0. We tested the 3 following hypotheses: in the meningeal/skull marrow ROI, whether the percentage of voxels showing increased <sup>11</sup>C-PBR28 uptake would (1) be higher over the visual cortex in migraineurs than in both control groups, (2) be similar over the other 3 cortical areas among all 3 groups, and (3) show a positive correlation with the number of visual aura episodes in the 4 weeks preceding the scan in the occipital PMT. We also tested whether the signal correlated with the number of migraine attacks (migraine with + without aura) in the past 4 weeks, and with number of days since the last attack.

**Statistical Analyses**

ANOVA and post hoc Tukey-corrected 2-tailed *t* tests were used to compare mean SUVR between the 3 groups. Data were

considered significant of *p* < 0.05, and we also report 95% confidence intervals (CIs). Spearman rho was used for the correlation analyses of the SUVR with (1) the number of visual aura episodes in the previous 4 weeks (with or without headache), as well as (2) the total number of migraine attacks in the previous 4 weeks and (3) the number of days before the scanning since the last attack. Unpaired *t* test was used to compare SUVR between migraineurs scanned shortly after their last migraine attack (0–7 days) versus later (8–18 days). Effect size was computed with Cohen *d* formula.

**Data Availability**

Anonymized data that support the findings of this study are available from the corresponding author upon reasonable request.

**Results**

Consistent with our hypotheses, we found elevated signal in the occipital PMT and not in the other 3 brain regions in migraineurs compared to other groups. Figure 2 illustrates the spatial distribution of SUVR in occipital cortex and in occipital PMT as represented in the average MNI brain. Compared with CLBP patients and healthy controls, MWA patients exhibited increased uptake in PMT overlying occipital cortex.

We then examined the signal in native space of individual patients. As shown in Figure 3, uptake could be observed overlying the meninges and in the skull area in 4 representative patients who had experienced migraine and visual auras. Enhanced PET signal was observed in nearly all patients<sup>14</sup> in primary visual cortex, bone marrow, and the expected vicinity of the meninges.

The histogram in Figure 4 shows a rightward skewed distribution of SUVR in MWA compared with CLBP and CON. These data reflect a higher uptake in occipital PMT in migraineurs compared with both other groups.

Note that within groups, there were no significant PET signal differences in the occipital PMT between the MABs and HABs (n = 4, n = 7, respectively; migraineurs:

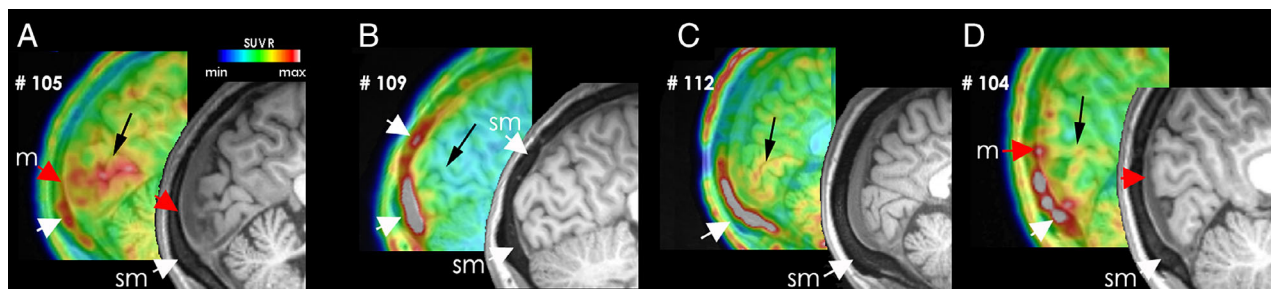


**FIGURE 3:** Native images of positron emission tomography (PET) tracer uptake in the skull marrow/meninges in original PET/magnetic resonance imaging data showing the occipital cortex and adjacent parameningeal tissues in 4 representative patients (#s). Black arrows indicate primary visual cortex; white arrows indicate bone marrow; red arrows indicate meninges. PET data are color-coded in a spectrum scale ranging from low (dark blue) to high (gray). m = location of meninges; sm = skull marrow; SUVR = standardized uptake value ratio.

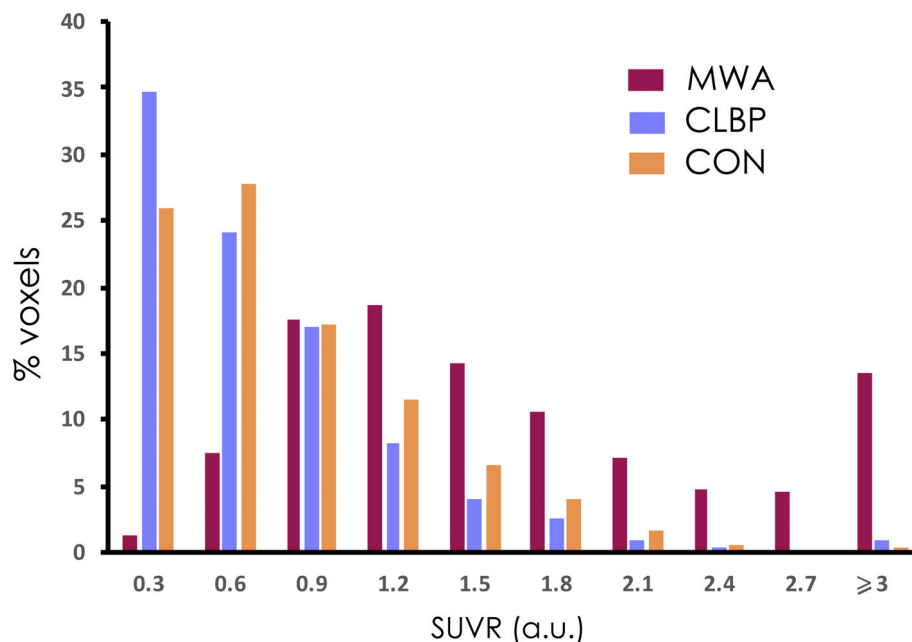


FIGURE 4: Histogram of distribution of the mean standardized uptake value ratio (SUVR) values (arbitrary units [a.u.]) in the occipital parameningeal tissues for migraineurs with aura (MWA), chronic low back pain patients (CLBP), and healthy controls (CON). Note the higher values of SUVRs (>1.2) in MWA compared to the other groups. [Color figure can be viewed at [www.annalsofneurology.org](http://www.annalsofneurology.org)]

$t = 0.71, p = 0.5$ ; CLBP  $t = 1.75, p = 0.1$ ; CON:  $t = 0.81, p = 0.44$ ).

We then examined whether this increased uptake was specific to the occipital PMT. A 4 (visual, orbitofrontal, DLPFC, and parietal) by 3 (migraineurs,

CLBP, CON) ANOVA evaluating SUVR group differences showed significant interaction ( $F_{6, 90} = 12.16, p < 0.0001$ ; Fig 5).

For the occipital PMT, Tukey multiple comparison test showed significant differences with large effect sizes

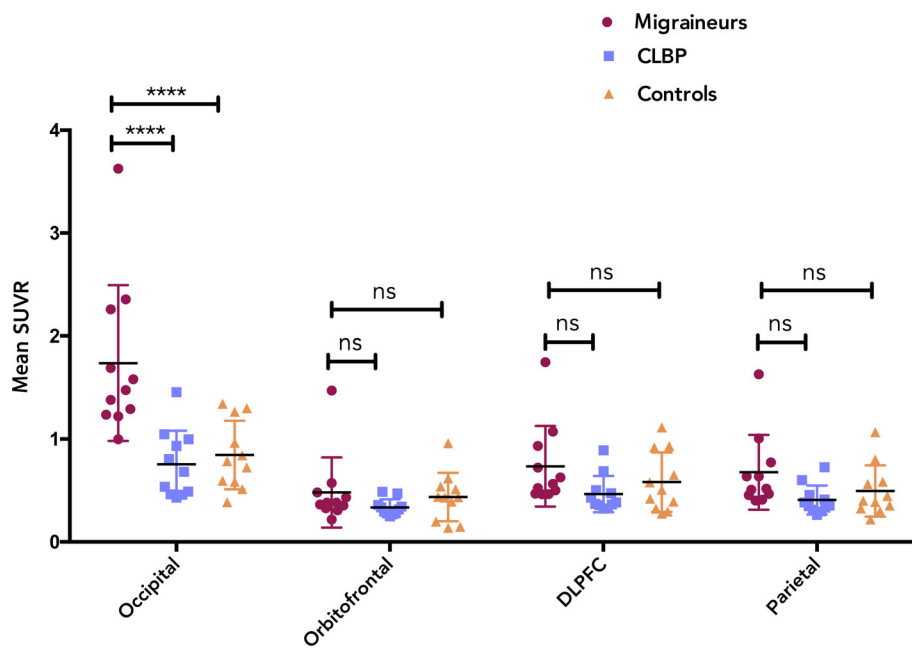


FIGURE 5: Mean standardized uptake value ratio (SUVR) values in each region of interest for each group in parameningeal tissues overlying the occipital, orbitofrontal, dorsolateral prefrontal cortex (DLPFC), and parietal regions. Values for migraineurs with aura (circles), chronic low back pain patients (CLBP; squares), and healthy controls (triangles) are shown. \*\*\*\*Statistically significant at  $p < 0.0001$ . ns = not significant. [Color figure can be viewed at [www.annalsofneurology.org](http://www.annalsofneurology.org)]



between MWA and CLBP and between MWA and CON ( $p < 0.0001$ , 95% CI = 0.65–1.32, Cohen  $d = 1.53$  and  $p < 0.0001$ , 95% CI = 0.56–1.28, Cohen  $d = 1.69$ , respectively). No differences were found when CLBP and CON were compared using Tukey multiple comparison test (not significant, 95% CI =  $-0.44$  to  $0.26$ ). For the orbitofrontal PMT, no significant differences were found between groups (MWA vs CLBP, 95% CI =  $-0.21$  to  $0.50$ ; MWA vs CON, 95% CI =  $-0.31$  to  $0.39$ ; CLBP vs CON, 95% CI =  $-0.45$  to  $0.25$ ). Similarly, for the DLPFC PMT, there were no significant differences between groups (MWA vs CLBP, 95% CI =  $-0.08$  to  $0.62$ ; MWA vs CON, 95% CI =  $-0.20$  to  $0.51$ ; CLBP vs CON, 95% CI =  $-0.47$  to  $0.23$ ) using Tukey multiple comparison test. Likewise, for the parietal PMT, Tukey multiple comparison test showed no significant differences between groups (MWA vs CLBP, 95% CI =  $-0.08$  to  $0.62$ ; MWA vs CON, 95% CI =  $-0.17$  to  $0.53$ ; CLBP vs CON, 95% CI =  $-0.44$  to  $0.26$ ).

We then tested the hypothesis that elevated tracer uptake in occipital PMT would correlate positively with the total number of visual auras. We found a statistically significant correlation between the mean SUVR and the total number of visual aura episodes (Spearman  $\rho = 0.74$ ,  $p = 0.01$ ).

There was, however, no significant correlation between PMT uptake and the total number of migraine attacks (with + without aura) in the previous 4 weeks ( $r = 0.14$ ,  $p = 0.7$ ). Moreover, there was no correlation between PMT uptake and the number of days since the last attack ( $r = 0.27$ ,  $p = 0.4$ ), and the enhanced uptake did not appear to diminish with time.

## Discussion

This study provides the first evidence of a persistent extra-axial inflammatory signal in a subtype of migraine, in patients with MWA. We found that (1) migraine with visual aura is associated with a sustained and enhanced inflammatory signal (ie, increased  $^{11}\text{C}$ -PBR28 binding reflecting increased TSPO expression) in a space occupied by meninges and bone (parameningeal [PMT] signal) overlying activated occipital cortex (also showing increased  $^{11}\text{C}$ -PBR28 binding, see Albrecht et al<sup>14</sup>); this uptake is greater in migraineurs than in both healthy control subjects and those with chronic low back pain, the latter condition also characterized by brain inflammation (Figs 2, 4, and 5)<sup>20</sup>; (2) by contrast, this increase in binding was not observed overlying the parietal, DLPFC, or orbitofrontal cortex (Fig 5); (3) the differences between  $^{11}\text{C}$ -PBR28 binding in migraineurs and CLBP patients suggest that the experience of pain may not necessarily be accompanied by PMT inflammation (Fig 5); and (4) the enhanced

PET signal in occipital PMT did not diminish with time, as there were no differences when comparing scans (SUVR) obtained 0 to 7 versus 8 to 18 days or 0 to 4 versus 14 to 18 days after the last attack. Taken together, these results are consistent with the conclusion that extra-axial inflammation is significantly augmented and prolonged in tissues overlying cortex generating visual aura. Our study offers evidence that PET imaging of an inflammatory signal provides a “historical fingerprint” of events during migraine with visual aura and identifies a phenotype of this migraine subtype.

We considered the merits of a time-dependent study but quickly realized that our study population (subjects with multiple episodes with short attack intervals during a 30-day period) was not ideal for such a study design. We now know this to be true, because we detected significant TSPO signal carryover between episodes that remained undiminished for even 18 days after the last attack (Patient #112). Therefore, without multiple scanning sessions (isotope injections) before and after attacks in each subject, time-dependent data would have been misleading. Nevertheless, the knowledge gained from studying these 11 patients, showing a robust and sustained signal enhancement, better informs us going forward regarding the proper design of a time-dependent study using multiple injections in subjects whose attack intervals are much less frequent (eg, 1 per month). Studying migraineurs with multiple episodes did maximize the possibility of detecting an enhanced inflammatory signal. Moreover, it also allowed us to establish a positive statistical relationship between signal enhancement and the number of visual aura episodes.

A site of extra-axial inflammation has not been identified previously in migraine patients. Clinically, aspirin and NSAIDs have long been used to treat migraine; steroids use has also been successful in some patients.<sup>21</sup> At the preclinical level, neurogenic inflammation has been well studied in migraine models and involves the release of vasoactive neuropeptides such as calcitonin gene-related peptide, pituitary adenylyl cyclase activating peptide, and substance P from trigeminovascular axons<sup>22</sup> that innervate the meninges<sup>23</sup> and the bone.<sup>24</sup> Other implicated inflammatory mediators include protons (acid-sensing ion channels), COX-2–generating prostaglandins and other cyclooxygenase products, serine proteases, nitric oxide (iNOS), and IL-6 as well as macrophages, dendritic cells, and mast cells.<sup>21,25–28</sup> Relevant to migraine aura, CSD generates proinflammatory prostaglandins and iNOS<sup>29</sup> and promotes mast cell degranulation,<sup>5,22</sup> meningeal edema,<sup>5,27</sup> and dilation of the middle meningeal artery, as well as macrophage and dendritic cell activation.<sup>6</sup>

Inflammation may be implicated even in migraine without aura. In 1 patient, extensive extravasation of technetium-99m–labeled human serum albumin was

observed over the convexity and in the epicenter of pain at 3 hours but not after 3 days.<sup>30</sup> Moreover, in a model that mimics a human model of migraine without aura,<sup>31</sup> dural macrophages started to express IL-1, IL-6, and iNOS, as mast cells degranulate hours after administering the triggering agent, nitroglycerin.<sup>32</sup>

It seems reasonable to accept the notion that meningeal inflammation contributes to the pathophysiology of photophobia and possibly phonophobia. All 11 migraineurs experienced photophobia. One proposed mechanism to explain it involves sensitization of trigeminovascular afferents and their downstream thalamic targets on neurons receiving converging inputs from the retina.<sup>33</sup> Much less is known about phonophobia, but it may involve similar mechanisms. What is less clear is the relationship of the enhanced PMT signal to pain, headache, and its history. Unlike the number of auras, there was no correlation between the number of headaches and SUVR, albeit headache intensity and duration were not considered. Importantly, however, TSPO has never been tested as a biomarker for pain, nor as a marker to reflect activity in primary afferent fibers. To more specifically address this complex relationship, scanning cohorts that experience visual auras without headache as well as that experience only migraine headache may prove useful.

### **Inflammation in Skull and Bone Marrow**

The extent of the inflammatory signal in calvarial bone was unanticipated. Colocalizing PET images with higher-resolution MRI indicates that this signal also includes the spongy layer of bone between the inner and outer skull table. This tissue contains hematopoietic bone marrow, a blood cell production site that also gives rise to inflammatory leukocytes. In meninges or bone marrow, there are numerous TSPO-expressing cell types that potentially could overexpress and thus provide enhanced binding sites. In the dura mater, these cells include macrophages, dendritic cells, and mast cells ([www.ImmGen.org](http://www.ImmGen.org)). In the bone marrow, they include macrophages, monocytes, myeloid progenitor cells, and neutrophils, although the latter does not feature in the classic repertoire of migraine-responding cell types. However, macrophages, mast cells, and dendritic cells have been implicated. In addition, TSPO is expressed in adipocytes or fat cells, and it is well established that adipocytes are a major source of multiple cytokines (eg, adiponectin).<sup>34,35</sup> Although not much is known, the process of age-dependent fat replacement of bone marrow is highly dynamic and the young migraine population under study could well have bone inflammatory signals emanating from adipocytes in addition to bone marrow cells, as by age 31 years (the mean age of our migraineurs), it has been shown that in trochanter and femur, 10% and 25% of the marrow is fat,

respectively.<sup>36</sup> In normal human skull, this process may be accelerated, although to our knowledge, specimens from patients with neuroinflammatory conditions have not been studied.

Whether the inflammatory signal migrates from underlying brain to meninges to bone marrow is of interest to us. Regarding microvascular channels, the skulls of both mice and also humans contain channels that may provide a bidirectional vascular bridge between meninges and skull bone marrow<sup>37</sup> and perhaps cortex.<sup>37,38</sup> Existing animal data suggest a centrifugally propagating signal from cortical gray matter to surrounding tissues, possibly via a cerebrospinal fluid (CSF) route,<sup>39</sup> via microvascular channels or depolarization of traversing trigeminal afferents,<sup>40</sup> or a combination of the above. In the mouse, these vascular channels are lined with endothelial cells, are approximately 20 $\mu$ m wide,<sup>37,38,41</sup> and express  $\alpha$ -SMA and the basement membrane protein laminin.<sup>38</sup> In humans, these vessels are estimated to be 100 $\mu$ m in diameter and may be part of the Haversian canal system.<sup>42</sup> After an inflammatory stimulus such as experimental meningitis or stroke, myeloid cells migrate through these channels from bone marrow toward the meninges and brain against the usual direction of blood flow (ie, away from brain).<sup>37,38</sup> The signal to bone marrow is not known but may come from upregulated cytokines and/or HMGB-1, an alarmin released from neurons during CSD<sup>29</sup> and stroke.<sup>43</sup> A second potential mechanism noted above involves signaling from proinflammatory neuropeptides released from sparsely distributed trigeminovascular axons that pass through the calvarium from the meninges.<sup>24</sup> Furthermore, there are recent examples of brain–bone marrow crosstalk that implicate connecting microvessels and possibly the lymphatic network in this process.<sup>41,44,45</sup> For example, in a model of acute lymphoblastic leukemia, bridging vessels provided the principal route for migrating lymphoblasts invading the subarachnoid space.<sup>38</sup>

Our data raise questions as to the role of bone and bone marrow in migraine with aura. We speculate that a sustained signal in the calvarium may serve as a local repository of inflammation and as a potential candidate to trigger subsequent attacks or possibly to promote migraine chronification. One recent case report of chronic migraine-like headache in a patient with petrous apicitis and its response to treatment<sup>46</sup> suggests that these relationships are worthy of additional studies.

### **Shortcomings**

One limitation of our study is that the 3 groups were not perfectly matched in terms of age and sex. To ensure that our results were not driven by demographic differences between groups, we computed statistics including only



females, as well as splitting the groups between younger (18–30 years old) and older participants. This did not change our results.

Some of our migraine subjects described disturbances in language, sensation, and speech during attacks (see Table), but these were too few to make any meaningful analysis. Sex differences were not explored. Furthermore, we did not measure blood or CSF for inflammatory markers. Some success in this direction was reported by sampling internal jugular blood.<sup>26</sup> In view of our data, these and other measurements bear expanding upon. For many reasons, migraine is not an easy disorder to study. These shortcomings notwithstanding, we anticipate that future studies will help to determine whether parameningeal inflammation is a distinguishing feature between different migraine subtypes and whether other extra-axial skull regions exhibit the responses we observed overlying visual cortex.

TSPO PET tracers have well-recognized limitations despite reports showing enhanced binding in brain parenchyma in brain diseases—including degenerative brain diseases (eg, Alzheimer disease, Parkinson disease, Huntington disease, amyotrophic lateral sclerosis, multiple sclerosis), stroke, and migraine—with likely inflammatory components (for review, see Alam et al<sup>47</sup>). It was recently used to image peripheral tissues such as immune cell infiltration in the bone after fracture,<sup>48</sup> inflamed pannus tissue in osteoarthritis, the activation of macrophage and stroma in the synovial tissue of patients with rheumatoid arthritis,<sup>49</sup> and in the neuroforamen of patients suffering from sciatica.<sup>50</sup> Our findings in migraine demonstrate that inflammation is consistently present in a pain-sensitive tissue, thereby reinforcing results from preclinical studies.<sup>5,51</sup> From our results, however, we cannot conclude whether the elevated TSPO signals observed in MWA patients reflect increased protein expression, increased cellular density, or both. On the other hand, the problem of nonspecificity of the ligand (ie, distinguishing among activated cell types) may have been advantageous here by boosting an inflammatory signal coming from multiple cell types.

Regarding the validity of the tracer, we were encouraged by a recent detailed report<sup>8</sup> finding a strong correlation between [<sup>3</sup>H]PBR28 radioligand binding in vitro (the tritiated version of the tracer we used) and the number of TSPO-positive cells across all CNS tissues examined. These include microglia and macrophages and also activated astrocytes (and in smaller measure endothelial cells) in vitro. Another limitation is that in the present study we did not perform kinetic modeling using a radiometabolite-corrected arterial input function, which is considered by some to be the gold standard for quantification of TSPO binding.

However, work from our group and others<sup>7,52,53</sup> suggests that semiquantitative ratio metrics may be similarly sensitive to detect pathology-related group differences in <sup>11</sup>C-PBR28 signal as classic kinetic modeling techniques. Nevertheless, future studies will need to validate the use of these metrics in migraine datasets.

In summary, this human study provides the first evidence for a robust and persistent inflammatory signal within PMT (meninges and bone marrow) overlying cortical areas generating migraine visual aura. These results in humans are compatible with conclusions from numerous animal model studies linking inflammation to CSD and may account for symptoms related to meningeal irritation. Finally, these findings raise important questions about the impact and consequences of an upregulated inflammatory signal in calvarium bone. They suggest that newly explored bridging vessels provide the conduits for possible signal migration from brain with implications for migraine pathophysiology as well as for the pathophysiology of other neuroinflammatory disorders (eg, head trauma, stroke, Alzheimer disease, multiple sclerosis).

---

## Acknowledgment

This work was supported by 5R21NS082926-02 (N.H.), 1P01AT009965 (V.N.), 01NS108419 (M.A.M., M.N.), NIH R01NS07832201 A1 (C.M.), and 1R01NS095937-01A1 (M.L.L.).

## Author Contributions

Study concept and design: N.H., C.M., C.G., M.L.L., M.A.M. Data acquisition and analysis: all authors. Drafting the text and figures: N.H., M.L.L., M.A.M.

## Potential Conflicts of Interests

Nothing to report.

---

## References

1. GBD 2016 Headache Collaborators. Global, regional, and national burden of migraine and tension-type headache, 1990–2016: a systematic analysis for the global burden of disease study 2016. *Lancet Neurol* 2018;17:954–976.
2. Hadjikhani N, Sanchez del Rio M, Wu O, et al. Mechanisms of migraine aura revealed by functional MRI in human visual cortex. *Proc Natl Acad Sci U S A* 2001;98:4687–4692.
3. Pietrobon D, Moskowitz MA. Pathophysiology of migraine. *Annu Rev Physiol* 2013;75:365–391.
4. Moskowitz MA, Nozaki K, Kraig RP. Neocortical spreading depression provokes the expression of c-fos protein-like immunoreactivity within trigeminal nucleus caudalis via trigeminovascular mechanisms. *J Neurosci* 1993;13:1167–1177.

5. Bolay H, Reuter U, Dunn AK, et al. Intrinsic brain activity triggers trigeminal meningeal afferents in a migraine model. *Nat Med* 2002;8:136–142.
6. Zhang X, Levy D, Nosedá R, et al. Activation of meningeal nociceptors by cortical spreading depression: implications for migraine with aura. *J Neurosci* 2010;30:8807–8814.
7. Albrecht DS, Granziera C, Hooker JM, Loggia ML. In vivo imaging of human neuroinflammation. *ACS Chem Neurosci* 2016;7:470–483.
8. Nutma E, Stephenson JA, Gorter RP, et al. A quantitative neuropathological assessment of translocator protein expression in multiple sclerosis. *Brain* 2019;142:3440–3455.
9. Cagnin A, Kassiou M, Meikle SR, Banati RB. Positron emission tomography imaging of neuroinflammation. *Neurotherapeutics* 2007;4:443–452.
10. Banati RB. Neuropathological imaging: in vivo detection of glial activation as a measure of disease and adaptive change in the brain. *Br Med Bull* 2003;65:121–131.
11. Cosenza-Nashat M, Zhao ML, Suh HS, et al. Expression of the translocator protein of 18 kDa by microglia, macrophages and astrocytes based on immunohistochemical localization in abnormal human brain. *Neuropathol Appl Neurobiol* 2009;35:306–328.
12. Rupprecht R, Papadopoulos V, Rammes G, et al. Translocator protein (18 kDa) (TSPO) as a therapeutic target for neurological and psychiatric disorders. *Nat Rev Drug Discov* 2010;9:971–988.
13. Lacor P, Benavides J, Ferzaz B. Enhanced expression of the peripheral benzodiazepine receptor (PBR) and its endogenous ligand octadecaneuropeptide (ODN) in the regenerating adult rat sciatic nerve. *Neurosci Lett* 1996;220:61–65.
14. Albrecht DS, Mainero C, Ichijo E, et al. Imaging of neuroinflammation in migraine with aura: a [(11)C]PBR28 PET/MRI study. *Neurology* 2019;92:e2038–e2050.
15. Cui Y, Takashima T, Takashima-Hirano M, et al. 11C-PK11195 PET for the in vivo evaluation of neuroinflammation in the rat brain after cortical spreading depression. *J Nucl Med* 2009;50:1904–1911.
16. Headache Classification Committee of the International Headache Society (IHS). The international classification of headache disorders, 3rd edition. *Cephalalgia* 2018;38:1–211.
17. Owen DR, Yeo AJ, Gunn RN, et al. An 18-kDa translocator protein (TSPO) polymorphism explains differences in binding affinity of the PET radioligand PBR28. *J Cereb Blood Flow Metab* 2012;32:1–5.
18. Hadjikhani N, Vincent M. *The Migraine Brain, Imaging Structure and Function*. Oxford, UK: Oxford University Press, 2012.
19. Izquierdo-García D, Hansen AE, Forster S, et al. An SPM8-based approach for attenuation correction combining segmentation and nonrigid template formation: application to simultaneous PET/MR brain imaging. *J Nucl Med* 2014;55:1825–1830.
20. Loggia ML, Chonde DB, Akeju O, et al. Evidence for brain glial activation in chronic pain patients. *Brain* 2015;138:604–615.
21. Waeber C, Moskowitz MA. Migraine as an inflammatory disorder. *Neurology* 2005;64:S9–S15.
22. Ashina M, Hansen JM, Do TP, et al. Migraine and the trigemino-vascular system—40 years and counting. *Lancet Neurol* 2019;18:795–804.
23. Mayberg M, Langer RS, Zervas NT, Moskowitz MA. Perivascular meningeal projections from cat trigeminal ganglia: possible pathway for vascular headaches in man. *Science* 1981;213:228–230.
24. Kosaras B, Jakubowski M, Kainz V, Burstein R. Sensory innervation of the calvarial bones of the mouse. *J Comp Neurol* 2009;515:331–348.
25. Conti P, D'Ovidio C, Conti C, et al. Progression in migraine: role of mast cells and pro-inflammatory and anti-inflammatory cytokines. *Eur J Pharmacol* 2019;844:87–94.
26. Sarchielli P, Floridi A, Mancini ML, et al. NF-kappaB activity and iNOS expression in monocytes from internal jugular blood of migraine without aura patients during attacks. *Cephalalgia* 2006;26:1071–1079.
27. Levy D. Endogenous mechanisms underlying the activation and sensitization of meningeal nociceptors: the role of immuno-vascular interactions and cortical spreading depression. *Curr Pain Headache Rep* 2012;16:270–277.
28. Reuter U, Chiarugi A, Bolay H, Moskowitz MA. Nuclear factor-kappaB as a molecular target for migraine therapy. *Ann Neurol* 2002;51:507–516.
29. Karatas H, Erdener SE, Gursoy-Ozdemir Y, et al. Spreading depression triggers headache by activating neuronal Panx1 channels. *Science* 2013;339:1092–1095.
30. Knotkova H, Pappagallo M. Imaging intracranial plasma extravasation in a migraine patient: a case report. *Pain Med* 2007;8:383–387.
31. Ashina M, Møller Hansen J, BO ÁD, Olesen J. Human models of migraine—short-term pain for long-term gain. *Nat Rev Neurol* 2017;13:713–724.
32. Reuter U, Bolay H, Jansen-Olesen I, et al. Delayed inflammation in rat meninges: implications for migraine pathophysiology. *Brain* 2001;124:2490–2502.
33. Nosedá R, Copenhagen D, Burstein R. Current understanding of photophobia, visual networks and headaches. *Cephalalgia* 2019;39:1623–1634.
34. Nishimura M, Izumiya Y, Higuchi A, et al. Adiponectin prevents cerebral ischemic injury through endothelial nitric oxide synthase dependent mechanisms. *Circulation* 2008;117:216–223.
35. Fantuzzi G. Adipose tissue, adipokines, and inflammation. *J Allergy Clin Immunol* 2005;115:911–919. quiz 20.
36. Tuljapurkar SR, McGuire TR, Brusnahan SK, et al. Changes in human bone marrow fat content associated with changes in hematopoietic stem cell numbers and cytokine levels with aging. *J Anat* 2011;219:574–581.
37. Herisson F, Frodermann V, Courties G, et al. Direct vascular channels connect skull bone marrow and the brain surface enabling myeloid cell migration. *Nat Neurosci* 2018;21:1209–1217.
38. Yao H, Price TT, Cantelli G, et al. Leukaemia hijacks a neural mechanism to invade the central nervous system. *Nature* 2018;560:55–60.
39. Plog BA, Nedergaard M. The glymphatic system in central nervous system health and disease: past, present, and future. *Annu Rev Pathol* 2018;13:379–394.
40. Strassman AM, Raymond SA, Burstein R. Sensitization of meningeal sensory neurons and the origin of headaches. *Nature* 1996;384:560–564.
41. Cai R, Pan C, Ghasemigharagoz A, et al. Panoptic imaging of transparent mice reveals whole-body neuronal projections and skull-meninges connections. *Nat Neurosci* 2019;22:317–327.
42. Saper CB, Jarowski CI. Leukemic infiltration of the cerebellum in acute myelomonocytic leukemia. *Neurology* 1982;32:77–80.
43. Roth S, Singh V, Tiedt S, et al. Brain-released alarmins and stress response synergize in accelerating atherosclerosis progression after stroke. *Sci Transl Med* 2018;10:piaa1313.
44. Rasmussen MK, Mestre H, Nedergaard M. The glymphatic pathway in neurological disorders. *Lancet Neurol* 2018;17:1016–1024.
45. Ahn JH, Cho H, Kim JH, et al. Meningeal lymphatic vessels at the skull base drain cerebrospinal fluid. *Nature* 2019;572:62–66.
46. Mancini AJ, Glassman RD, Chang YM, et al. Headache in petrous apicitis: a case report of chronic migraine-like headache due to peripheral pathology. *Headache* 2019;18:1821–1826.

47. Alam MM, Lee J, Lee SY. Recent progress in the development of TSPO PET ligands for neuroinflammation imaging in neurological diseases. *Nucl Med Mol Imaging* 2017;51:283–296.
48. Cropper HC, Johnson EM, Haight ES, et al. Longitudinal translocator protein-18 kDa-positron emission tomography imaging of peripheral and central myeloid cells in a mouse model of complex regional pain syndrome. *Pain* 2019;160:2136–2148.
49. Narayan N, Owen DR, Mandhair H, et al. Translocator protein as an imaging marker of macrophage and stromal activation in rheumatoid arthritis pannus. *J Nucl Med* 2018;59:1125–1132.
50. Albrecht DS, Ahmed SU, Kettner NW, et al. Neuroinflammation of the spinal cord and nerve roots in chronic radicular pain patients. *Pain* 2018;159:968–977.
51. Schain AJ, Melo-Carrillo A, Borsook D, et al. Activation of pial and dural macrophages and dendritic cells by cortical spreading depression. *Ann Neurol* 2018;83:508–521.
52. Herranz E, Gianni C, Louapre C, et al. Neuroinflammatory component of gray matter pathology in multiple sclerosis. *Ann Neurol* 2016;80:776–790.
53. Lyoo CH, Ikawa M, Liow JS, et al. Cerebellum can serve as a pseudo-reference region in Alzheimer disease to detect neuroinflammation measured with PET radioligand binding to translocator protein. *J Nucl Med* 2015;56:701–706.